Volume 1 | Number 1 | Jan 2013 | Pages 1–100

ChemComm

Chemical Communications
www.rsc.org/chemcomm

ROYAL SOCIETY OF CHEMISTRY

ROYAL SOCIETY OF CHEMISTRY

www.rsc.org/chemcomm

ChemComm

Journal Name

COMMUNICATION

Highly nitrogen doped carbon nanosheets as efficient electrocatalysts for oxygen reduction reaction

Lei Wang,[†a] Shuo Dou,[†b] Jiantie Xu,[c] Hua Kun Liu,[c] Shuangyin Wang,[b,]* Jianmin Ma[a,c,]* and Shixue Dou[c]

In this work, highly nitrogen doped carbon nanosheets (HNCNSs) have been successfully prepared by annealing EDTA calcium disodium salt, which exhibited a direct four-electron reaction pathway and high stability as efficient metal-free catalysts for oxygen reduction reaction.

Fuel cells are considered as the power plants with non-pollution, high efficiency, wide application, no noise, which play an important role in many areas of power, automotive, communications, and so on.[1, 2] However, practical application of fuel cells has been hindered largely by the slow kinetic of oxygen reduction reactions.[3-5] Although regarded as the best catalyst for the oxygen reduction reaction (ORR), Platinum (Pt) and Pt-based electrodes were still confined to its high cost, rarity of materials, diffusion of fuel molecules into theelectrodes andpoisoning.[6-8] Thence, the crucial issue in the development of fuel cells is the search for lower cost and more-stable electrocatalysts to replace Pt-based electrodes for ORR.

Recently, much research has indicated that the heteroatoms in carbon materials, such as N, S, and P, play a critical role in their electrocatalytic performance.[9-12] Thus, many efforts have focused on the introduction of heteroatoms into the carbon materials for achieving a high electrocatalytic activity. Especially, N-doped carbon materials had attracted much attention because of its high efficiency as metal-free electrocatalysts for ORR. Nitrogen doping methods have been well developed, such as chemical-vapour deposition (CVD) in the presence of N-containing precursors,[13-15] the thermal annealing with NH_3 and solvent-based preparation.[16, 17] Nevertheless, the low output and high cost of these synthetic methods limit their application only to basic research. Therefore, developing a low-cost and eco-friendly method is still of great interest.

In this work, we have successfully synthesized HNCNS (N: 18.96 wt %) by annealing low-cost, nitrogen-rich EDTA calcium disodium salt at 700 ^{o}C in Ar atmosphere. During increasing the temperature, EDTA calcium disodium salt decomposed into calcium carbonate and calcium oxide with gas evolution. The SEM of unpickled products was shown in **Fig. S1**. These intermediate products play an important role in the formation of sheet structure, as hard and soft support. Then, the remaining samples were immersed in a certain concentration of hydrochloric acid to obtaining HNCNSs finally. The FTIR spectra of the commercial EDTA calcium disodium salt and HNCNSs illustrated the complete decomposition of the precursor, as shown in **Fig. S2**. Also, SEM images of the samples synthesized at 600 and 800 °C were shown in **Fig. S3**, which had no uniform morphology. When tested as catalysts for ORR, the as-synthesized HNCNS electrodes had excellent electrocatalyticperformance in the alkaline electrolyte, thanks to high content of pyridinic N and pyrrolic N in HNCNSs.
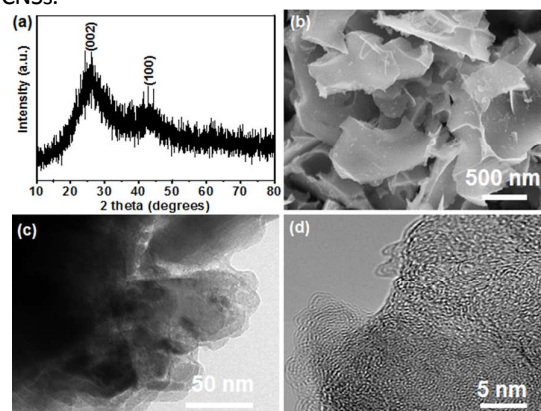
a. *Key Laboratory for Micro-/Nano- Optoelectronic Devices of the Ministry of Education, School of Physics and Electronics, Hunan University, Changsha 410082, P. R. China*

b. *State Key Laboratory of Chem-/Bio-Sensing and Chemometrics, College of Chemistry and Chemical Engineering, Hunan University, Changsha 410082, P. R. China*

c. *Institute for Superconducting and Electronic Materials, University of Wollongong, Wollongong, NSW 2522, Australia*

† Lei Wang and Shuo Dou have equal contributions to this work.
Electronic Supplementary Information (ESI) available: [Experimental section, Raman spectrum, and LSV curves of Pt/C catalyst]. See DOI: 10.1039/x0xx00000x

COMMUNICATION　　　　　　　　　　　　　　　　　　　　　　　　Journal Name

Fig. 1 (a) XRD pattern, (b) SEM image, (c) TEM image and (d) HR-TEM image of HNCNSs.

The XRD pattern of HNCNSs in **Fig. 1a** presents two broad peaks at 2θof about 26° and 43° corresponding to the (002) and (100) planes of carbon, respectively. Raman spectrum in **Fig. S4** presents two distinct peaks at ca.1322.5 cm^{-1} (D band) andca.1590.5 cm^{-1} (G band) of carbon, respectively. The D/G intensity ratio (I_D/I_G, 1.19) could indicates that there exists a lot of structural defects,[18-20] which are associated with a series of edges, other defects and disordered carbon. Scanning electron microscopy (SEM) and transmission electronmicroscopy (TEM) images were in **Fig. 1b and c** showed that the sample is composed of nanosheets. High magnification TEM (HR-TEM) image (**Fig. 1d**) that the nanosheet is amorphous carbon material. The EDX element maps of HNCNSs (**Fig. S5**) for the distribution of C, N, and O revealed that the C, N, and O elements were well-distributed in HNCNSs and exhibited no apparent element separation or aggregation.
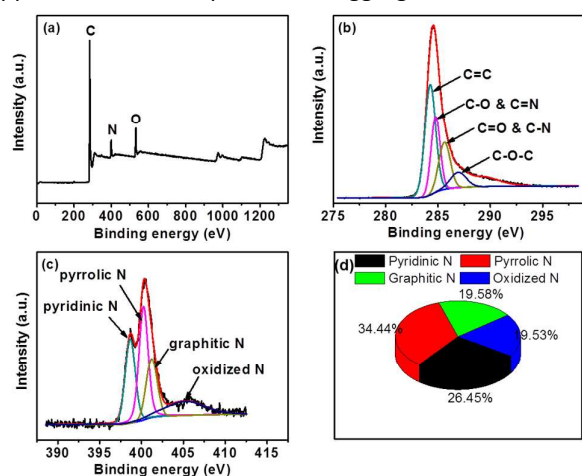

Fig. 2 The XPS spectra of HNC: (a) survey specrum; (b) high resolution XPS spectra of C1s; (c) high resolution XPS spectra of N1s; (d) the content rate of nitrogen functional groups.

X-ray photoelectron spectroscopy (XPS) was carried out to analyze the elemental compositions and nitrogen bonding forms of HNCNSs. **Fig. 2** shows three characteristic peaks at ca. 285, 400 and 532 eV, which corresponds to C1s, N1s and O1s, respectively. The content of C, N and O elements is 72.72 %, 18.96 % and 8.32 %, respectively. TheC1s spectrum will change when nitrogen atoms are doped into carbon.[21, 22] In the C1sspectrum of HNCNSs (**Fig. 2b**), the spectrum was deconvoluted to four individual peaks. The sharp peak at around 284.5 eV corresponds to C=C bonds, called sp^2 carbon, while the other peaks at higher energy accords to different C-O bonding configurations, C-O bonds and C=N bonds, C=O and C-N bonds, O-C=O bonds. **Fig. 2c** shows that the N1s XPS spectrum of HNCNSs. Generally, nitrogen functionalgroups in carbon catalysts are composed of four components: pyridinic N (398.7 eV), pyrrolic N (400.3 eV), quaternary N (graphitic N, 401.2 eV), and N-oxides ofpyridinic N (oxidized N, 402.8 eV).[23-27] Pyridinic N refers to N atoms at the edges of graphene planes. Pyrrolic N atoms

are incorporated into five-membered heterocyclic rings. Quaternary N atoms are incorporated into the graphene layer and substitute carbon atoms within the graphene plane. N-oxides of pyridinic N are N atoms bonded to two carbon atoms and one oxygen atom.[28-30] The content of pyridinic N, pyrrolic N, graphitic N and oxidized N in HNCNSs is 26.45 %, 34.44 %, 19.58 %, 19.54 %, respectively, as shown in**Fig.2d**. It is reported that the pyridinic N and pyrrolic N are active nitrogen atoms, which contribute to the ORR.[14, 31-33] HNCNSs with 11.55 % active nitrogen atoms are expected to display an effective electrocatalytic behavior.

Fourier transform IR (FTIR) spectroscopy was also measured to the chemical structure of HNCNSs. According to the FTIR spectra in **Fig. S2**, the HNCNSs contained -OH (at ac.3440 cm^{-1}), C-N (at ac.1340 cm^{-1}), C=N (at ac.1630 cm^{-1}) bonds, without -COOR bond (ester groups, at ac.3410 cm^{-1}) that appeared in the EDTA calcium disodium salt. The result illustrated the complete decomposition of ester groups and it was in accordance with XPS. The Brunauer-Emmett-Teller (BET) surface area of the HNCNSs was measured, as shown in **Fig. S6**. From the BET analysis and the porous size distributions, the specific surface area of HNCNSs was 85 m^{2}g^{-1} and the HNCNSs existed microporous. The formation of small pores resulted in the subsequent decomposition of EDTA calcium disodium salt along with gas release.
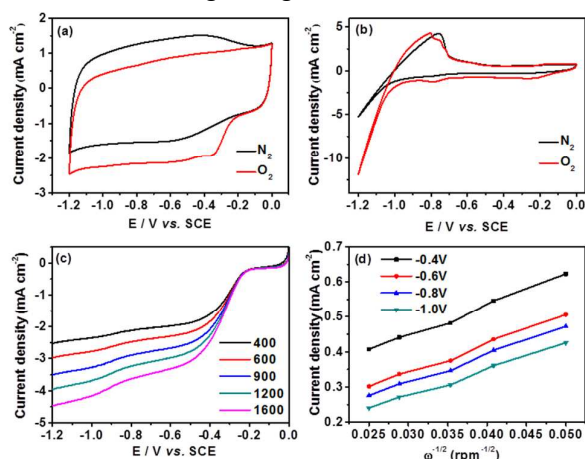

Fig. 3 (a and b)CV curves of HNCNSs and Pt/C at a scan rate of 50 mV s-1 in N$_2$-saturated and O$_2$-saturated aqueous solution of 0.1 M KOH, respectively; (c) LSV of HNCNSs in an O$_2$-saturated 0.1 M aqueous KOH solution with a scan rate of 10 mV s^{-1} at rotation rates from 400 to 1600 rpm; and (d) Koutecky–Levich plots of HNCNSs at different electrode potentials.

The catalytic activities of the as-synthesized HNCNSs for ORR were reflected by the following measurement, the cyclic voltammetry (CV), linear-sweep voltammetry (LSV) and rotating ring/disk electrode (RRDE). Cyclic voltammogram(CV) curves of HNC electrode were examined in N$_2$-saturatedandO$_2$-saturatedaqueoussolution of 0.1 M KOH at 50 mV s^{-1}. The CV curves of HNCNSs for ORR obtained in O$_2$-saturatedKOHsolution, which has an apparent reduction process, is quite different from the graph in N$_2$-saturatedaqueoussolution, as shown in **Fig. 3a**. There is no

Please do not adjust margins

ChemComm

Journal Name COMMUNICATION

obvious peak position for the CV curves in N_2-saturatedaqueoussolution. The reduction peak of HNC electrode is at -0.33V in the O_2-saturated electrolyte solution. The peak current density of HNCNSs electrode is superior to that of commercial Pt/C electrode (**Fig. 3b**),indicating a pronounced electrocatalytic activity of HNCNSs towards ORR. **Fig. 3c** presents the LSV curves of HNC in an O_2-saturated 0.1 M aqueous KOH solution with a scan rate of 10 mV s^{-1} at rotation rates from 400 to 1600 rpm. In addition, the LSV curves of HNCNSs and Pt/C in an O_2-saturated 0.1 M aqueous KOH solution with a scan rate of 10 mV s^{-1} at 1600 rpm are exhibited in **Fig. S7**. The polarization curves measured at a rotation rate of 1600 rpm indicated that the ORR onset potential on HNCNSs was more positive than that of the samples annealed at 600, 800℃, while the limiting diffusion current at -1.0 V of HNCNSs was stronger than others, which demonstrated that HNCNSs electrode had better catalytic performance. According to the Koutecky–Levich equation, [34] we calculated electron number (n) per O_2 for HNCNSs electrode is 3.2, 3.4, 3.5 and 3.8 at the potential of-0.4V, -0.6V, -0.8V, -1.0V, respectively, as shown in **Fig. 3d**.The ring and disc currents of HNCNSs and the commercial Pt/C electrodes obtained by RRDE measurement in an O_2-saturated 0.1 M aqueous KOH solution with a scan rate of 10 mV s^{-1} at 1600 rpm were shown in **Fig. S8**. The n value of HNCNSs calculated by RRDE technique was consistent with that of K-L equation. The results prove the oxygen reduction of HNCNSs follows the one step direct four electrons transfer pathway, which contributes highly efficient fuel cell.[35-37]

The stabilities and possible crossover effects of catalytic materials are also very important for practical applications, because fuel molecules (e.g., methanol) may pass through the membrane from anode to cathode and poison the cathode catalyst.[38-40] The cyclic voltammogram tests were measured in 0.1 M KOH containing 1.0 M of methanol for the HNCNSs and the commercial Pt/C (20%) electrocatalyst. The CV curves of HNCNSs and Pt/C at 100 mV s^{-1} in O_2-saturated 0.1 M KOH solution as well as O_2-saturated 0.1 M KOH solution with addition of 1.0 M methanol, as shown in **Fig. 4a and b**, respectively. The curves of HNCNSs show no obvious diversification with the addition of 1.0 M methanol. In contrast, the typical methanol oxidation behavior was observed on Pt/C in the presence of methanol in the electrolyte solution. At the same time, CV scanning was conducted in 0. 1 M KOH for 1000 cycles at a scan rate of 100 mV s^{-1}between -1.0V to 0 V, as shown in **Fig. 4c and d**. The current density and onset potentialof HNC electrode almost unchanged during continuous CV scanning. By comparison, the current density became smaller gradually and the onset potential shifted negatively obviously for Pt/C electrocatalyst. Therefore, the electrocatalytic activity of HNCNSs for ORR is much more stable than that of the commercial Pt/C.
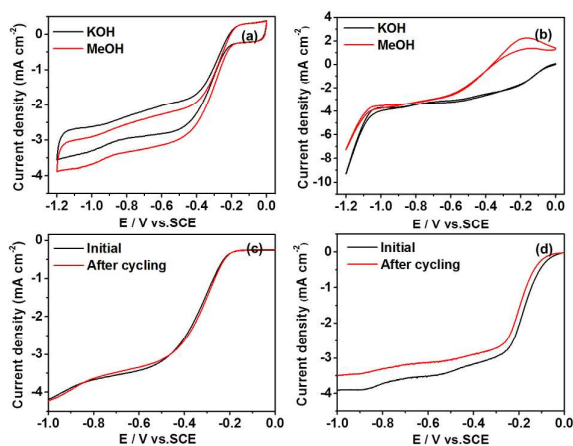

Fig. 4 The stability and possible methanol crossover effect: (a and b) CV curves of HNCNSs and Pt/C at 100 mV s^{-1} in O_2-saturated 0.1 M KOH solution as well as O_2-saturated 0.1 M KOH solution with addition of 1.0 M methanol; (c and d) the initial and 1000th cycle of LSV curves of HNC and Pt/C in aqueous 0.1M O_2-saturated KOH at 1600 rpm.

In summary, we have successfully developed a novel synthetic route to prepare HNCNSs by annealing EDTA calcium disodium salt in Ar atmosphere. When used as electrocatalyst, the as-prepared HNCNSs exhibited high catalytic activity towards ORR via direct $4e^{-1}$pathway, thanks to the structure to expose the rich active sites of high N-doped carbon. The HNCNSs is expected to be an effective and stable metal-free electrocatalysts in alkaline solutions.

Notes and references

‡Footnotes relating to the main text should appear here. These might include comments relevant to but not central to the matter under discussion, limited experimental and spectral data, and crystallographic data.
1   R. Bashyam and P. Zelenay, *Nature*,2006,**443**, 63-66.
2   M. Armand and J. M. Tarascon, *Nature*, 2008, **451**, 652-657.
3   K. Gong, F. Du, Z. Xia, M. Durstock and L. Dai, *Science*, 2009, **323**, 760-764.
4   J. Zhang,, K. Sasaki, E. Sutter and R. R. Adzic, *Science*, 2007, **315**, 220-222.
5   D. Pillay, M. D. Johannes, Y. Garsany and K. E. Swider-Lyons, *J. Phys. Chem. C*, 2010, **114**, 7822-7830.
6   H.B. Wang, T. Maiyalagan and X. Wang, *ACS Catal.*, 2012, **2**, 781-794.
7   M. K.Debe, *Nature*, 2012, **486**, 43-51.
8   A. A. Gewirth and M. S. Thorum, *Inorg.Chem.*, 2010, **49**, 3557-3566.
9   Z.Y. Lin, G. Waller, Y. Liu, M. L. Liu and C. P. Wong, *Adv. Energy Mater.*, 2012, **2**, 884-888.
10   J. Liang, Y. Jiao, M. Jaroniec and S. Z. Qiao, *Angew. Chem. Int. Ed.*, 2012, **51**, 11496-11500.
11   D.S. Yang, D. Bhattacharjya, S. Inamdar, J. Park and J. S.Yu, *J. Am. Chem. Soc.*, 2012, **134**, 16127-16130.

ChemComm Accepted Manuscript

12 T. Ikeda, M. Boero, S. F. Huang, K. Terakura, M. Oshima and J. Ozaki, *J. Phys. Chem. C*, 2008, **112**, 14706-14709.

13 Y. Q. Liu, D. C. Wei, Y. Wang, H. L. Zhang, L. P. Huang and G. Yu, *Nano Lett.*, 2009, **9**, 1752-1758.

14 L.T. Qu, Y. Liu, J. B. Baek and L. M. Dai, *ACS Nano*, 2010, 4, 1321-1326.

15 Z. Yang,Y. Xia and R. Mokaya, *Chem. Mater.*, 2005, **17**, 4502-4508.

16 X. L. Li, H. L. Wang, J. T. Robinson, H. Sanchez, G. Diankov and H. J. Dai, *J. Am. Chem. Soc.*, 2009,**131**, 15939-15944.

17 I. Y. Jeon, D. S. Yu, S. Y. Bae, H. J. Choi, D. W. Chang, L. M. Dai and J. B. Baek, *Chem. Mater.*, 2011, **23**, 3987-3992.

18 R.N. Singh and R. Awasthi, *Catal. Sci. Technol.*, 2011, **1**, 778-783.

19 W. Qian, R. Hao, Y. Hou, Y. Tian, C. Shen, H. Gao and X. Liang, *Nano Res*., 2009, **2**, 706-712.

20 Y. Zhou, Q. Bao, L. A. L. Tang, Y. Zhong and K. P. Loh, *Chem. Mater*., 2009, **21**, 2950–2956.

21 S. Wang, L. Zhang, Z. Xia, A. Roy, D. W. Chang, J. B. Baek, L. Dai, *Angew. Chem. Int. Ed.*, 2012, **51**, 4209-4212.

22 C. Z. Zhang, N. Mahmood, H. Yin, F. Liu and Y. L. Hou, *Adv. Mater.,*2013, **25**, 4932-4937.

23 Y. C. Lin, C. Y. Lin and P. W. Chiu, *Appl. Phys. Lett*., 2010, **96**, 133110.

24 D. H. Long , W. Li, L. C. Ling, J. Miyawaki, I. Mochida and S.H. Yoon, *Langmuir*, 2010, **26**, 16096-16102.

25 E. J. Biddinger and U. S. Ozkan, *J. Phys. Chem. C*, 2010, **114**, 15306.

26 S. Gupta, D. Tryk, I. Bae, W. Aldred and E. Yeager, *J. Appl. Electrochem*., 1989, **19**, 19-27.

27 R. Liu, D. Wu, X. Feng and K. Müllen, *Angew. Chem. Int. Ed.*, 2010, **49**, 2565-2569.

28 J.R. Pels, F. Kapteijin, J.A. Moulijin, Q. Zhu and K.M. Thomas, *Carbon*, 1995, **33**, 1641-1653.

29 S. Biniaka, G. Szymański, J. Siedlewskia and A. Switkowski, *Carbon*, 1997, **35**, 1799-1810.

30 W. Yue, J. G. Zhang, L. Wang, D. H. Wang, F.Ding, X. M.Tao and W. Chen, *Sci. Rep.*, 2013, **3**, 2771.

31 K. P. Gong, F. Du, Z. H. Xia, M. Durstock and L. M. Dai, *Science*, 2009, **323**, 760-764.

32 S. B. Yang, X. L. Feng, X. C. Wang and K. Müllen, *Angew. Chem. Int. Ed.*, 2011, **50**, 5339-5343.

33 Y. J. Zhang, K. Fugane, T. Mori, L. Niu and J. H. Ye, J. *Mater. Chem*., 2012, **22**, 6575-6580.

34 S. Y. Wang, D. S. Yu and L. M. Dai, *J. Am. Chem. Soc*.,2011, **133**, 5182-5185.

35 L. F. Lai, J. R. Potts, D. Zhan, L. Wang, C. K. Poh, C. H. Tang, H. Gong, Z. X. Shen, J. Y. Lin and R. S. Ruoff, *Energy Environ. Sci.*, 2012, **5**, 7936-7942.

36 L. P. Zhang and Z. H. Xia, *J. Phys. Chem. C,* 2011, **115**, 11170-11176.

37 R. A. Sidik, A. B. Anderson, N. P. Subramanian, S. P. Kumaraguru and B. N. Popov, *J. Phys. Chem. B*, 2006, **110**, 1787-1793.

38 M. N. Zhang, Y. M. Yan, K. P. Gong, L. Q. Mao, Z. X. Guo and Y. Chen, *Langmuir*, 2004, **20**, 8781-8785.

39 M. Neergat, A. K. Shukla and K. S. Gandhi, *Appl. Electrochem.*, 2001, **31**, 373-378.

40 Y. Tan, C. Xu, G. Chen, X. Fang, N. Zhen and Q. Xie, *Adv. Funct. Mater.*, 2012, **22**, 4584-4591.